Carbohydrate Polymers 74 (2008) 519–526

Contents lists available at ScienceDirect

Carbohydrate Polymers

journal homepage: www.elsevier.com/locate/carbpol

Dissolution kinetics of water-soluble polymers: The guar gum paradigm

Qi Wang [a], Peter R. Ellis [b], Simon B. Ross-Murphy [c,*]

[a] Food Research Program, AAFC, 93 Stone Road West, Guelph, Canada N1G 5C9
[b] King's College London, Nutritional Sciences Division, Biopolymers Group, Franklin-Wilkins Building, 150 Stamford Street, London SE1 9NH, UK
[c] King's College London, Pharmaceutical Sciences Research Division, Molecular Biophysics Group, Franklin-Wilkins Building, 150 Stamford Street, London SE1 9NH, UK

ARTICLE INFO

Article history:
Received 16 July 2007
Received in revised form 30 January 2008
Accepted 4 April 2008
Available online 11 April 2008

Keywords:
Guar gum
Galactomannan
Non-starch polysaccharides
Hydration
Dissolution kinetics
Ultimate viscosity
Particle size effects
Peppas model

ABSTRACT

The ability of many water/electrolyte soluble polymers (WSPs), such as guar galactomannan, to form molecular solutions when dispersed in water is important industrially, for example in food applications, and in controlling the release of drugs in the gastrointestinal tract. Certain WSPs, including guar, are also referred to generically as 'soluble fibre' and some of these fibre preparations are currently available on prescription in the UK and elsewhere. The functional and exploitational properties of such polymers are reliant on the solution viscosity, which is, in turn, dependent on the rate and extent of dissolution in the aqueous solvent. This work extends previous experimental work on the effect of particle size on the dissolution (hydration) rate of guar gum powders over a wide range of particle sizes. In this earlier work, the main experimental variable was the solution viscosity, but we extend this by calculating a new effective concentration from the viscosity and exploring the dissolution rates in terms of this variable. The advantages and limitations of this approach are discussed, and a number of dissolution models, some well known and others novel, are explored. These include t_{50}, diffusion limited and chemical kinetics models. In view of the results, we suggest because of the particulate size, the model based on chemical kinetics appears the most successful. Aqueous guar gum is a model "entanglement solution" system, so the work should have applicability to many other WSP systems.

1. Introduction

The ability of many water-soluble polymers (WSPs) such as guar galactomannan, to form molecular solutions when dispersed in water is of importance in a number of technological processes. In the pharmaceutical sector, for example, the functional properties of these polysaccharides are of importance for controlling the release of drugs in the gastrointestinal tract. (Chourasia & Jain, 2004; Friend, 2005; Montejo, Barcia, Fernandez-Carballido, & Molina-Martinez, 2004) Moreover, nutraceutical preparations that contain one or more water-soluble non-starch polysaccharides (NSPs) as the bioactive ingredient, are promoted commercially for their potential health benefits e.g. bulk-forming laxative and blood glucose-lowering effects in the treatment of diabetes. (Ellis & Morris, 1991; Guo, Skinner, Harcum, & Barnum, 1998; Judd & Ellis, 2006; Patrick, Gohman, Marx, DeLegge, & Greenberg, 1998; Slavin & Greenberg, 2003) Such water-soluble NSPs are often referred to generically as 'soluble fibre' in the medical and nutritional literature, and some fibre preparations are currently available on prescription in the UK. (Joint Formulary Committee, 2006) Water-soluble polymers are also used as excipients and bulking agents in a large number of formulations. "Viscosifying" guar gum solutions also occur in other applications. For example in the oil industry, guar gum and its derivatives are major ingredients in drilling muds and fingering fluids, (Goel, Shah, & Asadi, 2000; Kesavan & Prudhomme, 1992; Perez, Siquier, Ramirez, Muller, & Saez, 2004; Zhou & Shah, 2004) and in the textile industry they are employed as "sizes" to help to improve printing quality. (Kesavan & Prudhomme, 1992; Schneider & Sostar-Turk, 2003; Turk & Schneider, 2000).

A number of factors are known to influence the hydration or dissolution process of WSPs, including their molecular weight and final solution concentration. In our recent series of papers on the dissolution (hydration) of guar powders, (Wang, Ellis, & Ross-Murphy, 2002, 2003, 2006) we have confirmed that another major determinant of hydration kinetics is particle size, which reflects the changes in surface area exposed to water. Commercial samples tend to have a particle size typically in the range 40–80 μm, but in the last of these three publications (Wang et al., 2006) we used a range extended up to ~0.5 mm. Here, the (weight average) M_w was maintained (effectively) constant, as was the initial nominal, concentration of polymer in the particulate material, C_0. This is an important step, because it appears that many literature studies, including those involving tabletting (see below), have not been able to de-convolute the effects of particle size from those of molecular weight.

Although the present paper concentrates entirely on guar, this system is now accepted as a model water-soluble "viscosifying"

* Corresponding author. Tel.: +44 20 7848 4238; fax: +44 20 7848 4500.
E-mail address: simon.ross-murphy@kcl.ac.uk (S.B. Ross-Murphy).

0144-8617/$ - see front matter © 2008 Published by Elsevier Ltd.
doi:10.1016/j.carbpol.2008.04.006

or "thickening" polymer and the approach should serve as a standard for other WSPs, such as the cellulose ethers. Indeed the guar gum system is, to use an expression sadly somewhat over-employed – but here, we would argue, entirely appropriate – a paradigm. The literature evidence for this is extensive, but essentially goes back to work published by one of the current authors in the 1980s, where guar was demonstrated to be a model "entanglement solution" system. (Richardson & Ross-Murphy, 1987; Robinson, Ross-Murphy, & Morris, 1982) This work now seems to be part of the accepted canon.

Previously our studies have shown that development of (zero shear) viscosity on hydration of guar samples could be generalised on a single master curve by shifting the data appropriately along the time axis, as shown in Fig. 1. Central to the arguments developed in this paper is the consideration of this data in terms of the concentration of polysaccharide. Consequently, we re-examine the experimental data from our last paper, (Wang et al., 2006) but with a quite different emphasis.

In our earlier papers (Wang et al., 2002, 2003, 2006) we monitored the dissolution process purely in terms of the development of viscosity, and since this is published we give only essential details. To pre-empt the obvious question, why did we not simply follow the concentration with time, as is the convention standard for low molecular weight species particularly in the pharmaceutical area? Here we argued that, for these high molecular weight materials, the concentration, calculated by direct chemical analysis will not relate to fully hydrated material, so the value obtained will differ from that calculated from viscosity measurements, except for the "ultimate viscosity". This is the value defined here as the viscosity measured for fully hydrated material, after long times.

Indeed in an earlier paper (Wang et al., 2002) we explained why we adopted the procedure of fitting the viscosity directly, rather than the concentration of dissolved material. To quote directly: "this (monitoring the concentration) would be more appropriate from the viewpoint of conventional chemical kinetics, but even though we centrifuged the extracted samples to remove totally undissolved ("filler" phase) material, we still do not have an equilibrium system. In other words, the viscosity even after filtration has a complex contribution from molecularly dissolved polymer, supramolecular but essentially hydrated material and solvent, so the relationship between the measured viscosity at any time ($<\infty$) is not necessarily a direct one. Consequently the idea that we use the ultimate viscosity versus concentration plots to back calculate the concentration of molecularly dispersed material is one we dismissed fairly early on". To quote "we were not convinced there was, at any particular shear rate, a one-to-one mapping between concentration and the measured viscosity of the still hydrating system". (Wang et al., 2002) the evidence for much of the above comment, including the evidence for supramolecular structure and the nature of undissolved material, follows from our work using the so-called pressure cell method to generate molecular solutions. (Patel, Picout, Ross-Murphy, & Harding, 2006; Picout, Ross-Murphy, Errington, & Harding, 2001, 2003; Picout, Ross-Murphy, Jumel, & Harding, 2002).

However, what this does allow us to do now is to calculate values of what we define as C_{eff}, the effective concentration of the system contributing to this viscosity. This is evaluated from the (zero shear rate) solution viscosity and, in the present text, we explore its dependence on time, t. Accepting the hypothesis above, the relationship between C_{eff} and the nominal initial concentration C_0 is that generally $C_{eff} < C_0$, but that $C_{eff} \to C_0$ as the hydration time, $t \to \infty$.

Since this is not an experimental paper *per se* we have not given any more than nominal particulars; full details are given in the earlier publications. (Wang et al., 2002, 2003, 2006) We note that other workers have also used the time development of viscosity to follow dissolution (most references in the papers above). For example, a recent publication by Larsen and co-workers (Larsen, Gaserod, & Smidsrod, 2003) applies a similar technique to alginate polymers, but the sample M_w's are appreciably lower than those here (typically by >10×) so the viscosities are also markedly lower. One of the figures (their Fig. 2) also shows that log shear stress is proportional to polymer concentration – which suggests that their data are in the un-entangled, or dilute, regime. Under these circumstances it is likely that the above problems do not occur, and

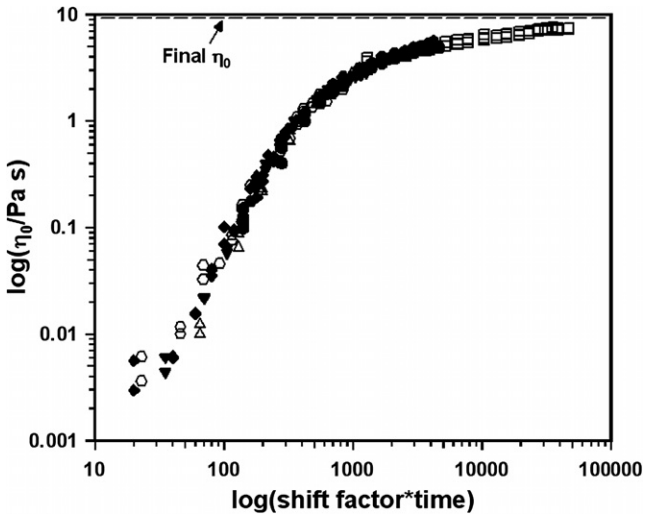

Fig. 1. Master curve of log viscosity versus scaled time, produced from viscosity versus time hydration data by applying shift-factor symbols: sample 1: filled diamond; sample 2: open hexagon; sample 3: filled triangle down; sample 4: open triangle up; sample 5: filled circle; sample 6: open square. Curves are cubic polynomial regressions to the means of the replicate measurements. Reproduced from Carbohydrate Polymers 64, 239–246 (2006) with permission from Elsevier Science.

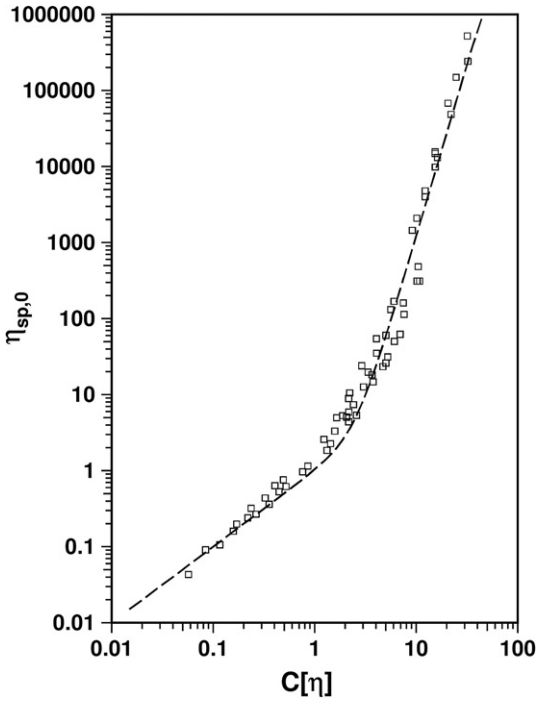

Fig. 2. Guar data from Robinson et al. (1982) plotted in the master plot form, and fitted to a modified Kulicke expression. The best fit, as is usual in this presentation, which spans 8 decades, corresponds to minimising the sum of squared of $\log(\eta_{sp,0})$ differences.

the viscosity at a given time can indeed be related directly to concentration.

Of course, the scenario above is rather different from those commonly in use in the pharmaceutical industry, since here polymeric materials usually occur as excipients in a compacted tablet. Under these circumstances, it appears the effect of particle size is rather different, and still not completely developed. For example one recent paper (Sumathi & Ray, 2003) using tamarind seed polysaccharide, TSP, a polymer which shares some characteristics with guar, (Picout et al., 2003) suggests that there is no particle size effect, at least in the range 43–250 μm, a result supporting earlier work.

However another paper (Agrawal, Neau, & Bonate, 2003) also using TSP, suggests that there is a particle size effect, but in the formed tablet this is the opposite of what we have seen. This work compares an ultra-fine particle size sample (ca. 10 μm) with a conventional sample (310 μm). Here the fine particle size sample appeared to slow the release rate (of, in this case, caffeine) compared to that of the larger size sample. This suggested that the smaller particle size sample allowed greater compaction (and binder efficiency) during the tabletting stage. Such an effect, which has been confirmed by other workers, has been attributed to a more rapid rate of wetting, leading to more rapid crossing of the glassy – "gel" layer boundary (Mitchell & Hartley, 1996) and subsequent formation of the diffusion-controlling gel layer around the tablet core. Interestingly we do not see the non-monotonic adsorption and dissolution rate behaviour predicted to occur in some solutions, from the effect of polymer disentanglement (Devotta, Ravetkar, Ambeskar, & Mashelkar, 1995). This is presumably because the product of C times $[\eta]$ is too high.

Overall what this also suggests, in that quite the opposite particle size dependence is seen for un-compacted materials, (Wang et al., 2006) is that there must be a "cross-over" at some intermediate degree of compaction. This may also be why the particle size effect is not seen for the larger particulate samples, and hints at a number of interesting future experiments. Experimentally, at least, the molecular weight effect appears less equivocal, with several papers suggesting, that in tablet dissolution studies, higher M_w slows release rate. (Durig, Lusvardi, & Harcum, 2004; Emeje, Kunle, & Ofoefule, 2006) This has even encouraged some workers (Korner, 2006; Korner, Larsson, Piculell, & Wittgren, 2005) to produce so-called "smart" blends of long and short chain length to control dissolution and release.

Several empirical dissolution models are discussed in the above papers, but there are also a number of more soundly based molecular models, including those for the dissolution of glassy polymers, which include dis-entanglement and reptation concepts. (Brochard & de Gennes, 1983; Narasimhan & Peppas, 1996) However, in the circumstance of our earlier work cited above, we found the latter not to be very helpful, and they are not discussed further here.

2. Results

2.1. Application of time shift method

We do not repeat the experimental details of the particle characterisation, hydration regime, and measurement of the viscosity, but refer the reader to the earlier papers, in particular Wang et al. (2006). The characteristics of the different particles are given here in Table 1; Fig. 1 shows the data re-scaled by multiplying the actual hydration times by an arbitrary factor. The time shift factor for the smallest particle size, for example, was found to be ≈130, with appropriate intermediate values, as given in Table 1, for the other samples.

What this meant in practice was that the viscosity developed by a sample hydrated for say 1 h, for the smallest particle size, was, within limitations, the same as that for the largest particle size sample when hydrated for 130 h, i.e. ≈5.4 days. Of course the assumption implicit in this approach is that the particles hydrate in a uniform manner and, in particular, do not fragment during the dissolution process under our conditions. This is because a mechanism of fragmentation and dispersion would tend to accelerate the overall hydration because dissolution occurs mainly at the particle surface and, given the same total volume, one very large particle would have a lower surface area than a number of smaller particles. Size and shape polydispersity would also have an effect, but this effect is also neglected. Fig. 1 is plotted in double logarithmic form, and the superposition suggests that, despite experimental errors, the reproducibility is generally high – only in certain cases can the repeated measurement values be distinguished.

However with these assumptions implicit, we expected the overall rate of hydration to depend on the surface area, for homogeneously shaped material, and on the volume for more tessellated and complex geometry particles. This suggested that the exponent for the time-scale for hydration should lie somewhere between 2 (since area $\propto d^2$) and 3 (volume $\propto d^3$), where d is the particle diameter. When we plotted the log of the time shift factor used in creating Fig. 1 against log(particle size), we obtained a linear plot and the exponent, calculated from the linear slope, was (−)2.46. (Wang et al., 2006) (The negative sign reflected that, perhaps contrary to intuition, we defined the time shift factor for the largest sample

Table 1
Moisture and galactomannan (GM) contents, intrinsic viscosity $[\eta]$, weight average molecular mass, M_w, mean particle size (d_{sv}), zero shear viscosity after 360 min hydration, η_{360}, final viscosity, η_∞ and "ultimate" C_{eff}, calculated (see text) from η_∞, for guar gum samples (numbered 1–6) of different particle size

Sample:	1	2	3	4	5	6
Moisture (%)	11.4	11.5	11.8	11.8	10.3	10.5
$[\eta]$ (dL/g)	16.1	16.7	16.9	16.4	17.3	16.0
M_w[c]	2.67×10^6	2.81×10^6	2.86×10^6	2.74×10^6	2.95×10^6	2.65×10^6
Galactomannan (%)	86.2	87.5	86.2	87.9	85.3	89.4
dsv (μm)	477	300	223	194	113	74
η_{360}/Pa s[a]	1.0_2	2.0_3	2.8_8	4.0_3	4.8_6[b]	7.3_8
η_∞/Pa s[a]	9.5_9	9.1_8	8.7_7	9.5_3	9.1_1	9.0_1
Time shift factor (Fig. 4b)	1	2.3	3.5	6.5	14	130
$C_{eff,\infty}$[d]/g dL^{-1}	0.98	0.94	0.92	0.96	0.90	0.97

Experimental values are means of 2–3 replicates.
[a] A subscripted figure indicates that the measured datum is not significant to better than 95% CI, i.e. 1.0_2 represents a value considered better than 1.0 ± 0.1 but not as precise as 1.02 ± 0.01.
[b] Value measured after 330 min.
[c] Calculated using Mark-Houwink parameters from Robinson et al. (1982) viz. $\alpha = 0.72$, $K' = 3.8 \times 10^{-4}$ g/dL.
[d] From ultimate viscosity, as dry weight.

to be unity. We did this in order to reflect an increase of the effective time-scale for the smallest sample.)

The advantage of the master curve approach appeared to us to be quite clear, in that we could interpolate the maximum (and intermediate) hydration time(s) for any particle size within this size range, ~70 to 500 μm, quite readily, and even use it to extrapolate to more extreme ranges.

2.2. Methods using the effective concentration, C_{eff} of hydrated material

If we wish to go further, and explore other possible "universalities" or master curves, then it would have to be, for example, via more traditional "chemical" kinetic routes, albeit as before that $C_{eff} \leqslant C_0$, where the equality condition applies only as time, $t \to \infty$.

2.2.1. Calculation of C_{eff}

Clearly in order to calculate C_{eff} from the zero shear viscosity η at any given time, we need some relationship between the two. Here we used the now essentially "standard" data of Robinson et al. (1982) in which the "space filling" parameter $C[\eta]$, with $[\eta]$ the intrinsic viscosity of the sample, was plotted against the specific viscosity η_{sp} for a whole range of different M_w guar samples at a range of concentrations (Fig. 2). (It is important to appreciate that although these data were for guar, as discussed elsewhere, (Morris, Cutler, Ross-Murphy, Rees, & Price, 1981) essentially the same "master curve" applies for a range of other water-soluble polymers, and even for the polymer solution "standard" polystyrene in toluene).

The initial difficulty is that, on passing through the entanglement concentration, the slope of these data shows a discontinuity, and no simple analytic form can be found that fits well, although attempts have been made; see e.g. Lapasin & Pricl (1995) for a summary of some of these. We have noted, however, (Ren, Ellis, Ross-Murphy, Wang, & Wood, 2003; Ren, Ellis, Sutherland, & Ross-Murphy, 2003) that a bridging function, simplified from that of Kulicke and Keniewske, (Kulicke & Keniewske, 1984) by defining the coefficient of the first term in the Kulicke expression, to be one, serves well. This equation then has the form:

$$\eta_{sp,0} = C[\eta] + a(C[\eta])^n \quad (1)$$

where

$$\eta_{sp,0} = \frac{\eta_0}{\eta_{solvent}} - 1 \quad (2)$$

Here the subscript zero indicates that values are measured at zero shear rate, and $\eta_{solvent}$ is the viscosity of, in this case, water.

There is no simple analytic solution for C in terms of Eqs. (1) and (2), because the best values of the parameters a and n for the Robinson guar data are ≈0.038 and 4.51, respectively. However, by equating the two right hand side terms, using $[\eta]$ values given in Table 1, $\eta_{solvent}$ = 1 mPa s, and these values of a and n, the resultant concentrations, now equal to our C_{eff}s, can be found for any given η using an iterative method. We used a simple 1-D bisection algorithm (Press, Flannery, Teukolsky, & Vetterling, 1986) with this, and the function in implicit form, both written as Visual Basic macros for Excel.

Encouragingly, even though we used a "look up table", relating concentration and viscosity that is now almost 25 years old, the estimates of the C_{eff}s for the different particle size samples from the respective ("infinite time") ultimate viscosities η_∞, are close to their nominal value, C_0, of 1.0 g dL, as shown in Table 1. Indeed, particularly in view of the approximations involved, these estimates, with a mean value of 0.94 g dL^{-1} and a standard deviation of 0.03, are very gratifying results.

2.3. Hydration rates using C_{eff} values

Applying the same method to previously published data generates a new figure, Fig. 3a, which obviously shows the same trends in behaviour as seen before, albeit that the data are less stretched for the ordinate, C_{eff} in Fig. 3a. This largely reflects the strong $C^{4.5}$ dependence of viscosity seen (cf. Fig. 2) for the majority of the data in this range. As in Fig. 1 we can replot this data in logarithmic form giving Fig. 3b. Unsurprisingly this looks quite similar to the un-superposed version of Fig. 1, and again can be re-superposed by multiplying time by an arbitrary factor, but since we have already assumed the two are functionally related in calculating the C_{eff}s, we decided not to pursue this approach.

There are, of course, a considerable number of dissolution models in the pharmaceutical literature, but almost all are concerned with the release of low M_w (i.e. < say 5×10^4) species, as is most relevant in this area. For higher molecular weight species, entanglement concepts will become relevant, as introduced above, and this would tend to limit their applicability. For this reason, we discuss only a few such models below.

2.4. Application of t_{50} models

A common way to quantify the release rate from a tablet is, of course, by the t_{50} value, that is, the time when 50% of the tablet material has been released into the surrounding dissolution medium. (Korner et al., 2005) Although we are interested in powders,

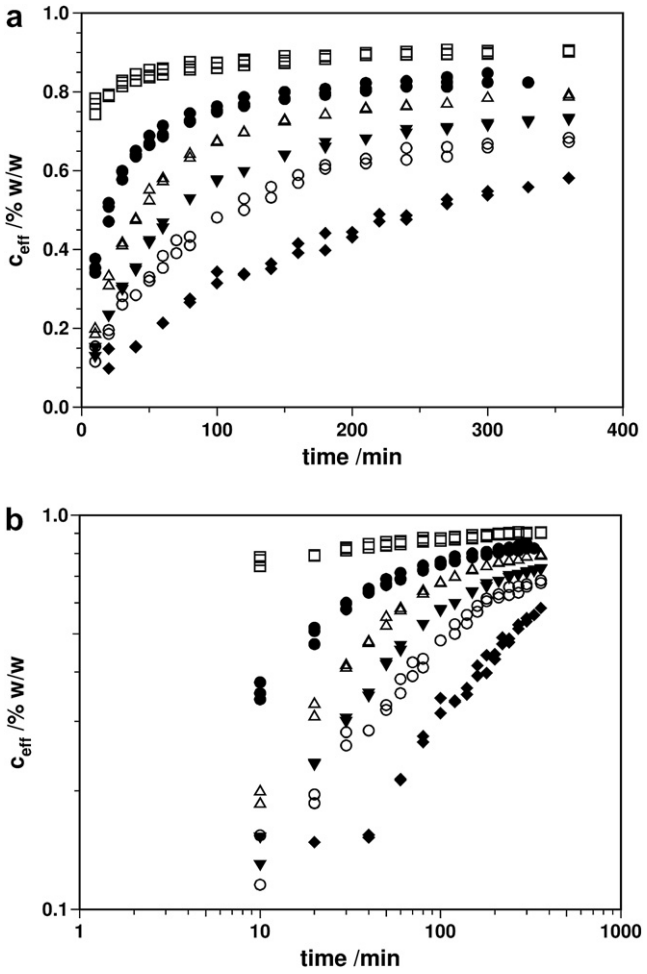

Fig. 3. (a) C_{eff} for all six samples plotted versus time t; symbols as Fig. 1. (b) As (a) but plotted with log time-scale.

rather than intact tablets, we decided to adopt this approach, but here t_{50} is defined as the time when C_{eff} is 50% of $C_{eff,\infty}$, given in Table 1. For the largest particle size samples, t_{50} can be estimated reasonably well from the raw data leading to Fig. 1. For the smallest, even the first datum corresponds to times well beyond this, so the value needs to be estimated, either by eye, or by using the polynomial fit.

However, many of the data in Fig. 4a are too close to the C_{eff} axis to help us examine the precise behaviour, so this is re-plotted as Fig. 4b with a $\log(t/t_{0.5})$ axis. In these plots we have not assumed, *a priori*, a value for the final concentration equivalent to η_∞ but, as discussed above, the values for all six samples superimpose reasonably well, and all are marginally below the C_0 of 1 g dL. What is even more interesting is if we now plot the t_{50} estimates against particle size. The slope (exponent) of this, Fig. 5, is 2.38 with a standard error of 0.03, very close to the value we found previously, (Wang et al., 2006) in the viscosity scaling mentioned above. However, it has to be said the slope is strongly influenced by the lowest point, where obtaining experimental data for t_{50} is difficult. If this point is excluded, regression statistics give a slope of 1.81 and a standard error of 0.08, closer to our original hypothesis that the behaviour would scale with surface area, i.e. that scaling multipliers such as t_{50} should be $\propto$ (particle size)^2.

In work on dissolution of discrete tablets, it is very common, in the usual linear time plot to see an initial concave region followed by one that is essentially linear, before the approach to the asymptote (Korner et al., 2005). Except for the possible exception of the two lowest points, where the experimental data are more unreliable, we saw no such effect, and this is presumably because of the lack of an initial, macroscopic tablet disintegration step. There will also be a faster equilibration in the mixing stage. In addition, this suggests that the breadth of the so-called swollen "gel" region surrounding the essentially un-hydrated particulate material is not so large (here the inverted commas reflect that, at least formally, this is a misuse of the term "gel", albeit that it is in common parlance in this area. For a more detailed discussion of this point, see, for example, Kavanagh & Ross-Murphy, 1998).

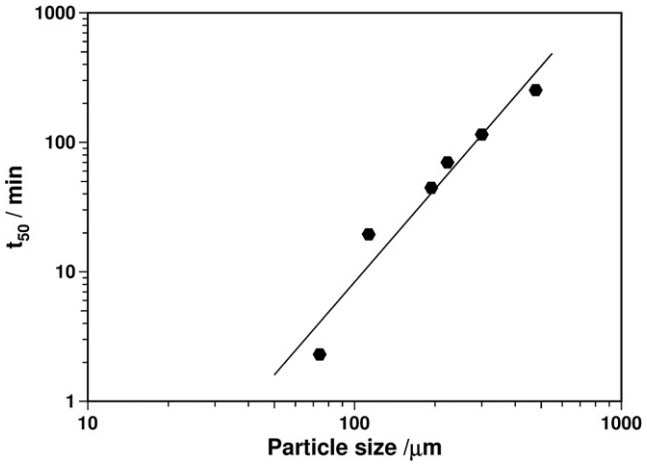

Fig. 5. t_{50}, 50% dissolution time plotted versus particle size. Slope is 2.38 with a standard error of 0.03.

As mentioned above, the guar samples still include intact cellular material, with the galactomannan mostly making up the cell wall material. (Ellis, Wang, Rayment, Ren, & Ross-Murphy, 2001) The smallest size sample (6 in Tables 1 and 2) is approximately the size of a single endosperm cell, whereas the other samples must be made up of clusters of cells. Hydration and dissolution of the polysaccharide may be assisted by this cellular structure, compared with the behaviour of a homogeneous powder.

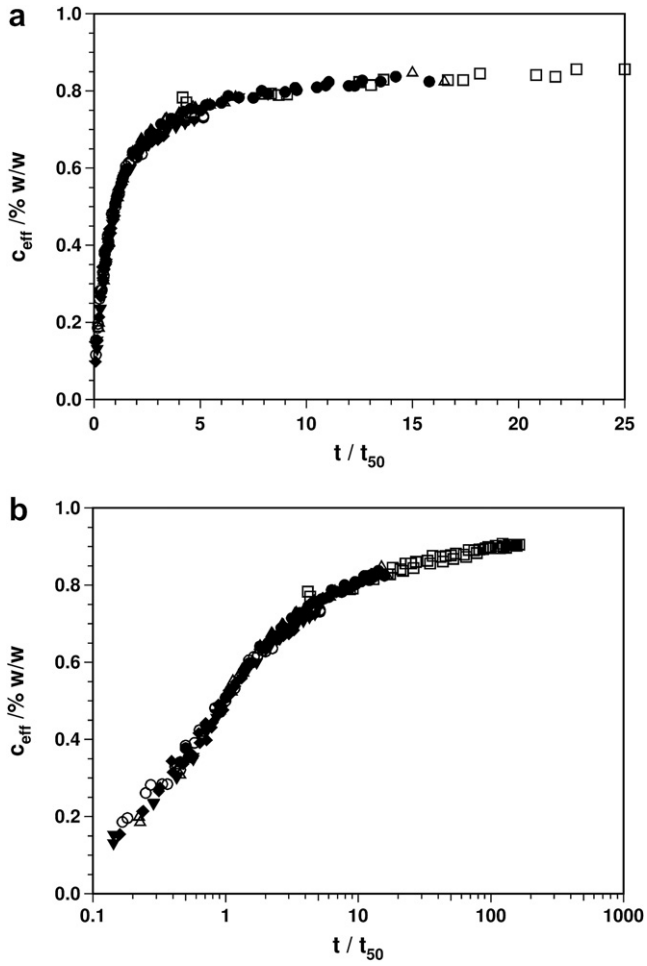

Fig. 4. (a) C_{eff} for all six samples plotted versus reduced time t/t_{50}; symbols as Fig. 1. (b) As (a) but plotted with log scale for t/t_{50}.

2.5. Diffusion controlled (Peppas type) models

We might therefore predict that the dissolution ("release") would be approximately Fickian, and so we would expect that the change in C_{eff} would be as shown by Eq. (3) with $n^* = 0.5$. (Higuchi, 1961; Peppas, 1985).

$$C_{eff}/C_0 = k' t^{n^*} \quad (3)$$

In fact this is certainly not the case, as can be seen by the "best" fits to this expression with a single rate constant shown in Fig. 6a. Even at a simple level this is a very poor model, because, as the figure shows, the predicted amount released C_{eff} soon becomes greater than the actual concentration of polymer, C_0. It also does not reproduce the rectilinear nature of the data, and for the small particle

Table 2
Best fit (least squares norm) parameters from Eqs. (3) and (4)

Sample:	1	2	3	4	5	6
d_{sv} (μm)	477	300	223	194	113	74
Peppas model, Eq. (3)						
n^*	0.54	0.39	0.34	0.28	0.18	0.05
k'	3.00E-02	8.00E-02	0.12	0.18	0.35	0.72
Kinetics model, Eq. (4)						
n'	2.55	2.62	2.39	2.54	2.32	4.15
k_n	5.3E-03	1.5E-02	2.2E-02	3.3E-02	8.6E-02	3.98

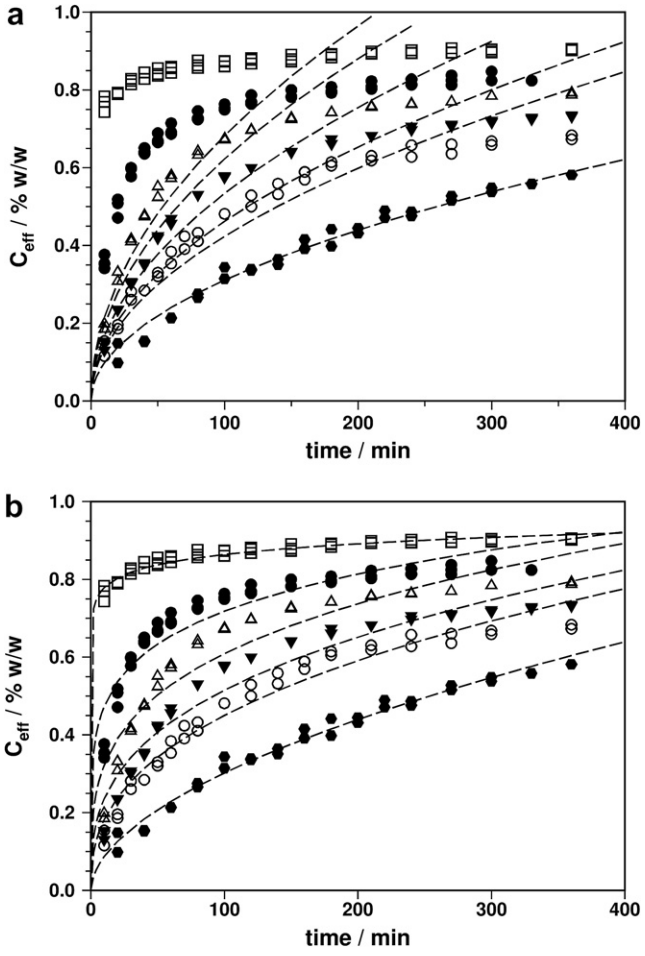

Fig. 6. (a) C_{eff} for all six samples plotted versus time; symbols as Fig. 1. Curves are best fits to Fickian $t^{1/2}$ dependence; (b) as (a) but plotted versus t^{n^*}. Exponent and rate constant as per Table 2.

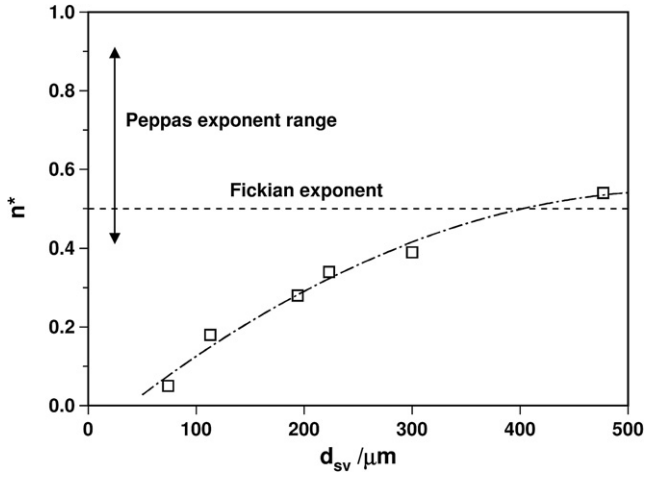

Fig. 7. Calculated values of the Peppas exponent n^* plotted against particle size (as d_{sv}). The dot dash line is a guide to the eye.

size samples, it is obviously unsatisfactory. Indeed only for the largest size sample (filled hexagons) does it provide anything like an acceptable fit. Clearly the process for the smaller particles is not simply, if at all, diffusion controlled.

For such systems the Peppas type equation form, in which n^* is allowed to vary (typically in the range 0.4–0.9 depending upon the mechanism of dissolution) has been widely applied. (Peppas, 1985; Peppas, Wu, & von Meerwall, 1994) Of course the fit from this (Fig. 6b) is much better than for the Fickian model since this introduces a second parameter, but the improvement is less clear than initial inspection of Fig. 6b would suggest. Firstly, there is again an unphysical indication that values of $C_{eff} > C_0$ can be obtained, and secondly the values of n^* are generally outside those usually expected, lying in the range 0.54 for the largest particle size sample, but decreasing monotonically to a value of 0.05 for the smallest (Table 2). Clearly, as the size of the particle decreases, the rate constant k′ increases, but in such a way that the product of k' and n^* is approximately constant, an interesting, but probably un-interpretable observation.

Values of n^* significantly less than 0.5 are not normally reported, and such a result almost certainly reflects the initial particle size, which is just too small for a (continuum) diffusion type expression to apply. As mentioned above, examination of Table 2 shows that an approximately Fickian exponent (0.54) is found for the particles of mean diameter ~0.5 mm. In fact plotting values of the n^* exponent against particle size (as shown in Fig. 7) shows a smooth evolution in behaviour. This we interpret by saying that a transition from microscopic to macroscopic behaviour occurs for particles around this size – an observation that seems intuitively attractive. This novel conclusion may also be of more particular significance, in view of the current interest in developing nano-sized high molecular weight particulate materials.

2.6. Models based on the nth order chemical kinetic equation

Since none of the above models was very successful for these microscopic particles, we decided to follow another approach. The form of the raw C_{eff} versus time data clearly suggests an appeal to a simple "chemical" kinetics model in which:

$$\frac{dC_{eff}}{dt} = -k_n C_{eff}^{n'} \quad (4)$$

This will clearly have the desired asymptotic behaviour that $C_{eff} \to C_0$ as $t \to \infty$, so the main concern is in the quality of fit, the reaction orders and the rate constants (we note here that it is the asymptotic shaped mathematical form of this equation we use, rather than suggesting any underlying physico-chemical model).

As Fig. 8 shows, the quality of fit is really very acceptable, and clearly much better than the Peppas n^* form, (Fig. 6b) with the same number of adjustable parameters. Examination of the n' "reaction order" parameters for the different particle size sets is also instructive, see Table 2. Here the value of n' appears essentially independent of particle size, (mean value 2.48, sd 0.12) except for the very smallest size sample (see comments below), and only the "rate constant" parameter, k_n changes – a much more acceptable behaviour. Indeed the values of the rate constants themselves demonstrate a quite reasonable and smoothly monotonic dependence on particle size (figure not shown). Fig. 8 also shows a line fitted to the smallest particle size in which n' has been constrained to have the mean value of 2.48 introduced above.

The latter fit is not particularly good, but the apparent rate constant is, at least, consistent with the values for the other sets. In chemical kinetics it is usual to relate the reaction order to the reaction mechanism. It is tempting to suggest that the apparent reaction order revealed here, at ~2.5 again suggests a mechanism in which dissolution lies between being particle surface area and volume controlled.

Interestingly the paper by Larsen and co-workers, on which we commented earlier, has obtained good results from a model that is essentially first order chemical kinetics. (Larsen et al., 2003) As we discussed, before their alginate systems generates much lower fi-

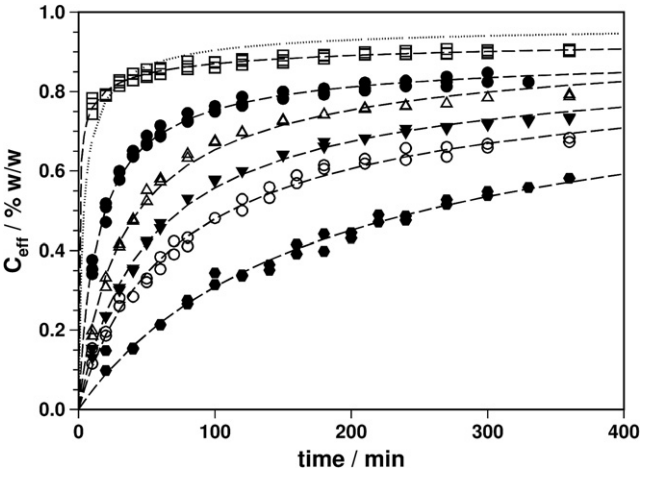

Fig. 8. C_{eff} for all six samples plotted versus time; symbols as Fig. 1 curves are best fits to the "chemical kinetics" model of Eq. (4); exponent and rate constant as Table 2. The dot dash line is the best fit for the smallest particle size sample, but with n' parameter constrained to be equal to the mean value, 2.48 ± 0.12 for the other five sets.

nal viscosities than ours, and the dissolution stage is far faster (a few minutes as opposed to several hours).

3. Discussion

Currently it appears there are very few models that can provide a relationship between particle size and dissolution rate in this particle size range, and most of these, as we discussed in our earlier papers, are quite limited. (Wang et al., 2002, 2003, 2006) The comparative simplicity of the approaches introduced above makes it potentially very attractive, and may prove of value for other high M_w particulate systems, in the pharmaceutical industry (such models also have applications in other areas e.g. oil extraction.) At this stage the work is clearly still at the hypothesis development stage. What now needs to be done is to repeat the measurement series and, most specifically, compare the actual concentration of material in "solution" albeit that it may not be "molecularly" dissolved (Picout et al., 2001, 2002) with that calculated from the solution of Eqs. (1) and (2). It may also be that this is the opportunity to recheck the now "classic" Robinson correlation, illustrated in Fig. 5. (Robinson et al., 1982) As far as applicability is concerned, it is very important that we exploit the generality implicit in such superposition approaches by examining other samples. An obvious candidate would be cellulose derivatives, since excellent model samples are now available, (Desbrieres, Hirrien, & Ross-Murphy, 2000) and such materials, albeit less well defined than the latter, are widely employed in the pharmaceutical sector.

A final, though very pertinent point is, of course, whether or not the results obtained previously, and treated here, depend upon the dissolution regime in the hydration "box", in particular the deformation/rate/regime – which will be a mixture of shear and extension. That is to say, whether or not the particle size dependence on the shift factors is independent of agitation conditions during hydration even within the range where particle fragmentation does not occur. The short answer is that only further experiments could answer this question, as we noted in our earlier publications (Wang et al., 2002, 2003, 2006).

On the other hand, even if this is a factor, it should not alter our main conclusions. That is because the present paper is intended to be much more about developing a series of approaches – many of them novel – in part, where not totally – for treating such a set of results, and obtaining insight without performing other experiments. That is of course, the strength of such superposition methods, and one we continue to espouse.

4. Conclusions

The models employed, and the several novel approaches developed here, have much broader relevance to the dissolution/hydration of other high molecular weight materials, which is why we regard these studies on the galactomannan guar as a model for other systems. Dissolution is a very important mechanism for any soluble material. The present work may have limited applicability to the vast literature of dissolution of conventional tablets. We suggest this is because at least one interpretation of the essential simplicity of the results obtained here, and their apparent "universality" suggests that dissolution of powders, even including those with a particle size approaching 0.5 mm involves fewer processes than the shell/gel type model commonly suggested. To investigate this in detail remains a task for future work.

Acknowledgements

The authors gratefully acknowledge the interest of, and support from Dr. Graham Sworn of Danisco, and to Mr. W.C. Wielinga, previously Meyhall Chemicals AG, Switzerland for preparing the samples. We also thank colleagues at King's College London, in particular Dr. A. Brain for the SEM work, Mr. V. Dawes, and Dr. X.M. Zeng for particle sizing methods, and both Dr. David Picout and Prof. Jayne Lawrence for valuable comments on an earlier draft, and for providing a number of helpful references. We also express gratitude to Prof. Lennart Piculell of Lund University, Sweden for providing a copy of the Ph.D. thesis of Dr. Anna Korner, and Prof. Olav Smidsrod of NTNU, Trondheim, Norway for constructive correspondence.

References

Agrawal, A. M., Neau, S. H., & Bonate, P. L. (2003). Wet granulation fine particle ethylcellulose tablets: Effect of production variables and mathematical modeling of drug release. *American Association of Pharmaceutical Scientists Journal, 5*, 1–13.

Brochard, F., & de Gennes, P. G. (1983). Kinetics of polymer dissolution. *Physicochemical Hydrodynamics, 4*, 313–322.

Chourasia, M. K., & Jain, S. K. (2004). Potential of guar gum microspheres for target specific drug release to colon. *Journal of Drug Targeting, 12*, 435–442.

Desbrieres, J., Hirrien, M., & Ross-Murphy, S. B. (2000). Thermogelation of methylcellulose: Rheological considerations. *Polymer, 41*, 2451–2461.

Devotta, I., Ravetkar, D. D., Ambeskar, V. D., & Mashelkar, R. A. (1995). A new phenomenological model for adsorption-diffusion in polymer solutions: Role of disengagement dynamics. *Chemical Engineering Science, 50*, 1129–1142.

Durig, T., Lusvardi, K. M., & Harcum, W. W. (2004). Hydroxypropylcellulose in modified release systems: Polymer molecular weight controls drug release rate and mechanism. *Hercules Aqualon Pharmaceutical Technical Report*, PTR-029, pp. 1–8.

Ellis, P. R., Wang, Q., Rayment, P., Ren, Y., & Ross-Murphy, S. B. (2001). Guar gum – agricultural and botanical aspects, physicochemical and nutritional properties, and its use in the development of functional foods. In S. S. Cho & M. Dreher (Eds.), *Handbook of dietary fiber* (pp. 613–657). New York: Marcel Dekker.

Ellis, P. R., & Morris, E. R. (1991). Importance of the rate of hydration of pharmaceutical preparations of guar gum – a new in vitro monitoring method. *Diabetic Medicine, 8*, 378–381.

Emeje, M. O., Kunle, O. O., & Ofoefule, S. I. (2006). Effect of the molecular size of carboxymethylcellulose and some polymers on the sustained release of theophylline from a hydrophilic matrix. *Acta Pharmaceutica, 56*, 325–335.

Friend, D. R. (2005). New oral delivery systems for treatment of inflammatory bowel disease. *Advanced Drug Delivery Reviews, 57*, 247–265.

Goel, N., Shah, S. N., & Asadi, M. (2000). New empirical correlation to predict apparent viscosity of borate-crosslinked guar gel in fractures. *S.P.E. Production & Facilities, 15*, 90–95.

Guo, J. H., Skinner, G. W., Harcum, W. W., & Barnum, P. E. (1998). Pharmaceutical applications of naturally occurring water-soluble polymers. *Pharmaceutical Science & Technology Today, 1*, 254–261.

Higuchi, T. (1961). Rate of release of medicaments from ointment bases containing drugs in suspension. *Journal of Pharmaceutical Science, 50*, 874–875.

Joint Formulary Committee. (2006). *British national formulary*. London, UK: British Medical Association and Royal Pharmaceutical Society of Great Britain.

Judd, P. A., & Ellis, P. R. (2006). Plant polysaccharides in the prevention and treatment of diabetes mellitus. In A. Suomyanath (Ed.), *Traditional medicine for modern times* (pp. 257–272). Boca Raton, FL, USA: Taylor and Francis Group.

Kavanagh, G. M., & Ross-Murphy, S. B. (1998). Rheological characterisation of polymer gels. *Progress in Polymer Science, 23*, 533–562.

Kesavan, S., & Prudhomme, R. K. (1992). Rheology of guar and HPG cross-linked by borate. *Macromolecules, 25*, 2026–2032.

Korner, A. (2006). Dissolution of polydisperse polymers in water. Ph.D. Thesis Lund University, Sweden.

Korner, A., Larsson, A., Piculell, L., & Wittgren, B. (2005). Tuning the polymer release from hydrophilic matrix tablets by mixing short and long matrix polymers. *Journal of Pharmaceutical Sciences, 94*, 759–769.

Kulicke, W. M., & Keniewske, R. (1984). The shear viscosity dependence on concentration, molecular weight and shear rate of polystyrene solutions. *Rheologica Acta, 23*, 75–83.

Lapasin, R., & Pricl, S. (1995). *Rheology of industrial polysaccharides: Theory and applications*. Glasgow, UK: Blackie Academic and Professional.

Larsen, C. K., Gaserod, O., & Smidsrod, O. (2003). A novel method for measuring hydration and dissolution kinetics of alginate powders. *Carbohydrate Polymers, 51*, 125–134.

Mitchell, J. R., & Hartley, L. (1996). The influence of water on the mobility, structure and dispersibility of hydrocolloids. In G. O. Phillips, P. A. Williams, & D. J. Wedlock (Eds.), *Gums and stabilisers for the food industry 8* (pp. 3–15). Oxford, U.K: Oxford University Press.

Montejo, C., Barcia, E., Fernandez-Carballido, A., & Molina-Martinez, I. T. (2004). Time delay avoids interaction between guar gum and sulphadiazine after oral administration. *Journal of Drug Delivery Science and Technology, 14*, 395–399.

Morris, E. R., Cutler, A. N., Ross-Murphy, S. B., Rees, D. A., & Price, J. (1981). Concentration and shear rate dependence of viscosity in random coil polysaccharide solutions. *Carbohydrate Polymers, 1*, 5–21.

Narasimhan, B., & Peppas, N. A. (1996). On the importance of chain reptation in models of dissolution of glassy polymers. *Macromolecules, 29*, 3283–3291.

Patel, T. R., Picout, D. R., Ross-Murphy, S. B., & Harding, S. E. (2006). Pressure cell assisted solution characterisation of galactomannans 3. Application of analytical ultracentrifugation techniques. *Biomacromolecules, 7*, 3513–3520.

Patrick, P. G., Gohman, S. M., Marx, S. C., DeLegge, M. H., & Greenberg, N. A. (1998). Effect of supplements of partially hydrolyzed guar gum on the occurrence of constipation and use of laxative agents. *Journal of the American Dietetic Association, 98*, 912–914.

Peppas, N. A. (1985). Analysis of Fickian and non-Fickian drug release from polymers. *Pharmaceutica Acta Helvetiae, 60*, 110–111.

Peppas, N. A., Wu, J. C., & von Meerwall, E. D. (1994). Mathematical-modeling and experimental characterization of polymer dissolution. *Macromolecules, 27*, 5626–5638.

Perez, R. M., Siquier, S., Ramirez, N., Muller, A. J., & Saez, A. E. (2004). Non-Newtonian annular vertical flow of sand suspensions in aqueous solutions of guar gum. *Journal of Petroleum Science and Engineering, 44*, 317–331.

Picout, D. R., Ross-Murphy, S. B., Errington, N., & Harding, S. E. (2001). Pressure cell assisted solution characterisation of polysaccharides I: Guar gum. *Biomacromolecules, 2*, 1301–1309.

Picout, D. R., Ross-Murphy, S. B., Errington, N., & Harding, S. E. (2003). Pressure cell assisted solubilization of xyloglucans: Tamarind seed polysaccharide and detarium. *Biomacromolecules, 4*, 799–807.

Picout, D. R., Ross-Murphy, S. B., Jumel, K., & Harding, S. E. (2002). Pressure cell assisted solution characterisation of polysaccharides 2: Locust bean gum and tara gum. *Biomacromolecules, 3*, 761–767.

Press, W. H., Flannery, B. P., Teukolsky, S. A., & Vetterling, W. T. (1986). *Numerical recipes*. Cambridge, U.K.: Cambridge University Press.

Ren, Y., Ellis, P. R., Ross-Murphy, S. B., Wang, Q., & Wood, P. J. (2003). Dilute and semi-dilute solution properties of (1-3), (1-4) β-D-glucan, the endosperm cell wall polysaccharide of oats (*Avena sativa* L.). *Carbohydrate Polymers, 53*, 401–408.

Ren, Y., Ellis, P. R., Sutherland, I. W., & Ross-Murphy, S. B. (2003). Dilute and semi-dilute solution properties of an exopolysaccharide from *Escherichia coli* strain S61. *Carbohydrate Polymers, 52*, 189–195.

Richardson, R. K., & Ross-Murphy, S. B. (1987). Nonlinear viscoelasticity of polysaccharide solutions. 1. Guar galactomannan solutions. *International Journal of Biological Macromolecules, 9*, 250–256.

Robinson, G., Ross-Murphy, S. B., & Morris, E. R. (1982). Viscosity molecular-weight relationships, intrinsic chain flexibility, and dynamic solution properties of guar galactomannan. *Carbohydrate Research, 107*, 17–32.

Schneider, R., & Sostar-Turk, S. (2003). Good quality printing with reactive dyes using guar gum and biodegradable additives. *Dyes and Pigments, 57*, 7–14.

Slavin, J. L., & Greenberg, N. A. (2003). Partially hydrolyzed guar gum: Clinical nutrition uses. *Nutrition, 19*, 549–552.

Sumathi, S., & Ray, A. R. (2003). Role of modulating factors on release of caffeine from tamarind seed polysaccharide tablets. *Trends in Biomaterials and Artificial Organs, 17*, 41–46.

Turk, S. S., & Schneider, R. (2000). Printing properties of a high substituted guar gum and its mixture with alginate. *Dyes and Pigments, 47*, 269–275.

Wang, Q., Ellis, P. R., & Ross-Murphy, S. B. (2002). Dissolution kinetics of guar gum powders. I. Methods for commercial polydisperse samples. *Carbohydrate Polymers, 49*, 131–137.

Wang, Q., Ellis, P. R., & Ross-Murphy, S. B. (2003). Dissolution kinetics of guar gum powders II. Effects of concentration and molecular weight. *Carbohydrate Polymers, 53*, 75–83.

Wang, Q., Ellis, P. R., & Ross-Murphy, S. B. (2006). Dissolution kinetics of guar gum powders III. Effect of particle size. *Carbohydrate Polymers, 64*, 239–246.

Zhou, Y. X., & Shah, S. N. (2004). Rheological properties and frictional pressure loss of drilling, completion, and stimulation fluids in coiled tubing. *Journal of Fluids Engineering-Transactions of the ASME, 126*, 153–161.